

We are IntechOpen, the world's leading publisher of Open Access books Built by scientists, for scientists

6,900

Open access books available

186,000

International authors and editors

200M

Downloads

Our authors are among the

154

Countries delivered to

TOP 1%

most cited scientists

12.2%

Contributors from top 500 universities



WEB OF SCIENCE™

Selection of our books indexed in the Book Citation Index
in Web of Science™ Core Collection (BKCI)

Interested in publishing with us?
Contact book.department@intechopen.com

Numbers displayed above are based on latest data collected.
For more information visit www.intechopen.com



Outage Performance and Symbol Error Rate Analysis of L-Branch Maximal-Ratio Combiner for κ - μ and η - μ Fading

Mirza Milišić, Mirza Hamza and Mesud Hadžialić
*Faculty of Electrical Engineering, University of Sarajevo
 Bosnia and Herzegovina*

1. Introduction

This chapter treats performances of Maximal-Ratio Combiner (MRC) in presence of two general fading distributions, the κ - μ distribution and the η - μ distribution (Yacoub, 2007.). Namely, performances of Maximal-Ratio Combiner in fading channels have been of interest for a long time, which can be seen by a numerous publications concerning this topic. Most of these papers are concerned by Rayleigh, Nakagami- m , Hoyt (Nakagami- q), Rice (Nakagami- n) and Weibull fading (Kim et al., 2003), (Annamalai et al., 2002), (da Costa et al., 2005), (Fraidenraich et al., a, 2005), and (Fraidenraich et al., b, 2005). Beside MRC, performances of selection combining, equal-gain combining, hybrid combining and switched combining in fading channels have also been studied. Most of the papers treating diversity combining have examined only dual-branch combining because of the inability to obtain closed-form expressions for evaluated parameters of diversity system. Scenarios of correlated fading in combiner's branches have also been examined in numerous papers. Nevertheless, depending on system used and combiner's implementation, one must take care of resources available at the receiver, such as: space, frequency, complexity, etc. Moreover, fading statistic doesn't necessary have to be the same in each branch, e.g. probability density function (PDF) can be the same, but with different parameters (Nakagami- m fading in i -th and j -th branches, with $m_i \neq m_j$), or probability density functions (PDF) in different branches are different (Nakagami- m fading in i -th branch, and Rice fading in j -th branch). This chapter treats MRC outage performances in presence of κ - μ and η - μ distributed fading (Milišić et al., a, 2008), (Milišić et al., b, 2008), (Milišić et al., a, 2009) and (Milišić et al., b, 2009). This types of fading have been chosen because they include, as special cases, Nakagami- m and Nakagami- n (Rice) fading, and their entire special cases as well (e.g. Rayleigh and one-sided Gaussian fading). It will be shown that the sum of κ - μ squares is a κ - μ square as well (but with different parameters), which is an ideal choice for MRC analysis. This also applies to η - μ distribution. Throughout this chapter probability of outage and average symbol error rate, at the L-branch Maximal-Ratio Combiner's output, will be analyzed. Chapter will be organized as follows.

In the first part of the chapter we will present κ - μ and η - μ distributions, their importance, physical models, derivation of the probability density function, and relationships to other commonly used distributions. Namely, these distributions are fully characterized in terms of

measurable physical parameters. The κ - μ distribution includes Rice (Nakagami- n), Nakagami- m , Rayleigh, and One-Sided Gaussian distributions as special cases. The η - μ distribution includes the Hoyt (Nakagami- q), Nakagami- m , Rayleigh, and One-Sided Gaussian distributions as special cases. In particular, κ - μ distribution better suites line-of-sight scenarios, whereas η - μ distribution gives better results for non-line-of-sight scenarios. Second part of this chapter will treat L-branch Maximal-Ratio Combiner and it's operational characteristics. We treat Maximal-Ratio Combiner because it has been shown that MRC receiver is the optimal multichannel receiver, regardless of fading statistics in various diversity branches since it results in a ML receiver. In this part of the chapter we will use the same framework used for derivation of κ - μ and η - μ probability density functions to derive probability density functions at combiner's output for κ - μ and η - μ fading. Derived probability density function will be used to obtain outage probability at combiner's output. In third part of the chapter analysis of symbol error rate, at combiner's output, will be conducted. This analysis will be carried out for coherent and non-coherent detection. Although coherent detection results in smaller error probability than corresponding non-coherent detection for the same average signal-to-noise ratio, sometimes it is suitable to perform non-coherent detection depending on receiver structure complexity. In this part of the chapter we will derive and analyze average symbol error probability for κ - μ and η - μ fading at combiner's output, based upon two generic expressions for symbol error probability for coherent and non-coherent detection types for various modulation techniques.

In fourth part we will discuss Maximal-Ratio Combiner's performances obtained by Monte Carlo simulations. Theoretical expressions for outage probability and average symbol error rate probability for κ - μ and η - μ fading will be compared to results of the simulations. We will also draw some conclusions, and some suggestions for future work that needs to be done in this field of engineering.

2. The κ - μ distribution and the η - μ distribution

2.1 The κ - μ distribution

The κ - μ distribution is a general fading distribution that can be used to better represent the small-scale variations of the fading signal in a Line-of-Sight (LoS) conditions. The fading model for the κ - μ distribution considers a signal composed of clusters of multipath waves, propagating in a nonhomogenous environment. Within single cluster, the phases of the scattered waves are random and have similar delay times, with delay-time spreads of different clusters being relatively large. It is assumed that the clusters of multipath waves have scattered waves with identical powers, and that each cluster has a dominant component with arbitrary power. Given the physical model for the κ - μ distribution, the envelope R , and instantaneous power P_R can be written in terms of the in-phase and quadrature components of the fading signal as:

$$R^2 = P_R = \sum_{i=1}^n (X_i + p_i)^2 + \sum_{i=1}^n (Y_i + q_i)^2 \quad (1)$$

, where X_i and Y_i are mutually independent Gaussian processes with $\overline{X_i} = \overline{Y_i} = 0$ and $\overline{X_i^2} = \overline{Y_i^2} = \sigma^2$. p_i and q_i are respectively the mean values of the in-phase and quadrature components of the multipath waves of cluster i , and n is the number of clusters of multipath.

Total power of the i -th cluster is $P_{R,i} = R_i^2 = (X_i + p_i)^2 + (Y_i + q_i)^2$. Since $P_{R,i}$ equals to the sum of two non-central Gaussian random variables (RVs), its Moment Generating Function (MGF), in accordance to (Abramowitz and Stegun, 1972, eq. 29.3.81), yields in:

$$M_{P_{R,i}}(s) = \frac{\exp\left(\frac{d_i^2 \cdot s}{1 - 2\sigma^2 \cdot s}\right)}{1 - 2\sigma^2 \cdot s} \quad (2)$$

, where $d_i^2 = p_i^2 + q_i^2$, and s is the complex frequency. Knowing that the $P_{R,i}$, $i=1,2,\dots,n$, are independent RVs, the MGF of the $f_{P_R}(P_R)$, where $P_R = \sum_{i=1}^n P_{R,i}$, is found to be:

$$M_{P_R}(s) = \prod_{i=1}^n M_{P_{R,i}}(s) = \frac{\exp\left(\frac{sd^2}{1 - 2s\sigma^2}\right)}{(1 - 2s\sigma^2)^n} \quad (3)$$

, where $d^2 = \sum_{i=1}^n d_i^2$. The inverse of (3) is given by (Abramowitz and Stegun, 1972, eq. 29.3.81):

$$f_{P_R}(P_R) = \frac{1}{2\sigma^2} \cdot \left(\frac{P_R}{d^2}\right)^{\frac{n-1}{2}} \cdot \exp\left(-\frac{P_R + d^2}{2\sigma^2}\right) \cdot I_{n-1}\left(\frac{d\sqrt{P_R}}{\sigma^2}\right) \quad (4)$$

It can be seen that $\Omega = \overline{R^2} = \overline{P_R} = 2n\sigma^2 + d^2$, and $\overline{R^4} = \overline{P_R^2} = 4n\sigma^4 + 4\sigma^2 d^2 + (2n\sigma^2 + d^2)^2$. We define $\kappa = \frac{d^2}{2n\sigma^2}$ as the ratio between the total power of the dominant components and the total power of the scattered waves. Therefore we obtain:

$$\frac{(\overline{R^2})^2}{\overline{R^4} - (\overline{R^2})^2} = \frac{(\overline{\gamma})^2}{\overline{P_R^2} - (\overline{P_R})^2} = n \cdot \frac{(1 + \kappa)^2}{(1 + 2\kappa)} \quad (5)$$

From (5), note that n may be expressed in terms of physical parameters, such as mean-squared value of the power, the variance of the power, and the ratio of the total power of the dominant components and the total power of the scattered waves. Note also, that whereas these physical parameters are of a continuous nature, n is of a discrete nature. It is plausible to presume that if these parameters are to be obtained by field measurements, their ratios, as defined in (5), will certainly lead to figures that may depart from the exact n . Several reasons exist for this. One of them, and probably the most meaningful, is that although the model proposed here is general, it is in fact an approximate solution to the so-called random phase problem, as are all the other well-known fading models approximate solutions to the random phase problem. The limitation of the model can be made less stringent by defining μ to be:

$$\mu = \frac{(\overline{R^2})^2}{\overline{R^4} - (\overline{R^2})^2} \cdot \frac{(1 + 2\kappa)}{(1 + \kappa)^2} = \frac{(\overline{\gamma})^2}{\overline{P_R^2} - (\overline{P_R})^2} \cdot \frac{(1 + 2\kappa)}{(1 + \kappa)^2} \quad (6)$$

with μ being the real extension of n . Non-integer values of the parameter μ may account for:

- non-Gaussian nature of the in-phase and quadrature components of each cluster of the fading signal,
- non-zero correlation among the clusters of multipath components,
- non-zero correlation between in-phase and quadrature components within each cluster, etc.

Non-integer values of clusters have been found in practice, and are extensively reported in the literature, e.g. (Asplund et al., 2002.). Using the definitions for parameters κ and μ , and the considerations as given above, the κ - μ power PDF can be written from (4) as:

$$f_{P_R}(P_R) = \frac{\mu(1+\kappa)^{\frac{\mu+1}{2}}}{\kappa^{\frac{\mu-1}{2}} \cdot \exp(\mu\kappa) \cdot \Omega^{\frac{\mu+1}{2}}} \cdot P_R^{\frac{\mu-1}{2}} \cdot \exp\left[-\frac{\mu(1+\kappa)P_R}{\Omega}\right] \cdot I_{\mu-1}\left[2\mu\sqrt{\frac{\kappa(1+\kappa)P_R}{\Omega}}\right]. \quad (7)$$

Therefore, the κ - μ envelope PDF can be obtained from (7) as:

$$f_R(R) = \frac{2\mu \cdot (1+\kappa)^{\frac{\mu+1}{2}} \cdot R^\mu}{\kappa^{\frac{\mu-1}{2}} \cdot \exp(\mu\kappa) \cdot \Omega^{\frac{\mu+1}{2}}} \cdot \exp\left[-\frac{\mu \cdot (1+\kappa) \cdot R^2}{\Omega}\right] \cdot I_{\mu-1}\left[2\mu \cdot \sqrt{\frac{\kappa \cdot (1+\kappa)}{\Omega}} \cdot R\right] \quad (8)$$

Instantaneous and average signal-to-noise ratio (SNR) are given by: $\gamma = \frac{P_R}{N_0} = \frac{R^2}{N_0}$, $\bar{\gamma} = \frac{\bar{P}_R}{N_0} = \frac{\Omega}{N_0}$, and therefore the κ - μ SNR PDF can be obtained from (8) as:

$$f_\gamma(\gamma) = \frac{\mu \cdot (1+\kappa)^{\frac{\mu+1}{2}} \cdot \gamma^{\frac{\mu-1}{2}}}{\kappa^{\frac{\mu-1}{2}} \cdot \exp(\mu\kappa) \cdot (\bar{\gamma})^{\frac{\mu+1}{2}}} \cdot \exp\left[-\frac{\mu \cdot (1+\kappa) \cdot \gamma}{\bar{\gamma}}\right] \cdot I_{\mu-1}\left[2\mu \cdot \sqrt{\frac{\kappa \cdot (1+\kappa) \cdot \gamma}{\bar{\gamma}}}\right] \quad (9)$$

N_0 represents single-sided power spectral density of additive white Gaussian noise. From (9) we can derive Cumulative Distribution Function (CDF) of instantaneous SNR as:

$$F_\gamma(\gamma) = \int_0^\gamma f_\gamma(t) dt = 1 - Q_\mu\left[\sqrt{2\kappa\mu}, \sqrt{\frac{2(\kappa+1)\mu\gamma}{\Omega}}\right] \quad (10)$$

, where Q stands for generalized Marcum- Q function defined in (Marcum, 1947.) as:

$Q_\nu(a, b) = \frac{1}{a^{\nu-1}} \int_b^\infty x^\nu \cdot \exp\left(-\frac{x^2 + a^2}{2}\right) \cdot I_{\nu-1}(ax) \cdot dx$. Now we can obtain closed-form expression for the n -th order moment of RV γ as:

$$\bar{\gamma}^n = \frac{\Gamma(\mu+n)}{\Gamma(\mu)\exp(\kappa\mu)} \cdot \left(\frac{\bar{\gamma}}{(1+\kappa)\mu}\right)^n \cdot {}_1F_1(\mu+n; \mu; \kappa\mu) \quad (11)$$

, where $\Gamma(\bullet)$ stands for gamma function (Abramowitz and Stegun, 1972, eq. 6.1.1), and ${}_1F_1(\bullet; \bullet; \bullet)$ represents confluent hypergeometric function (Abramowitz and Stegun, 1972, eq. 13.1.2).

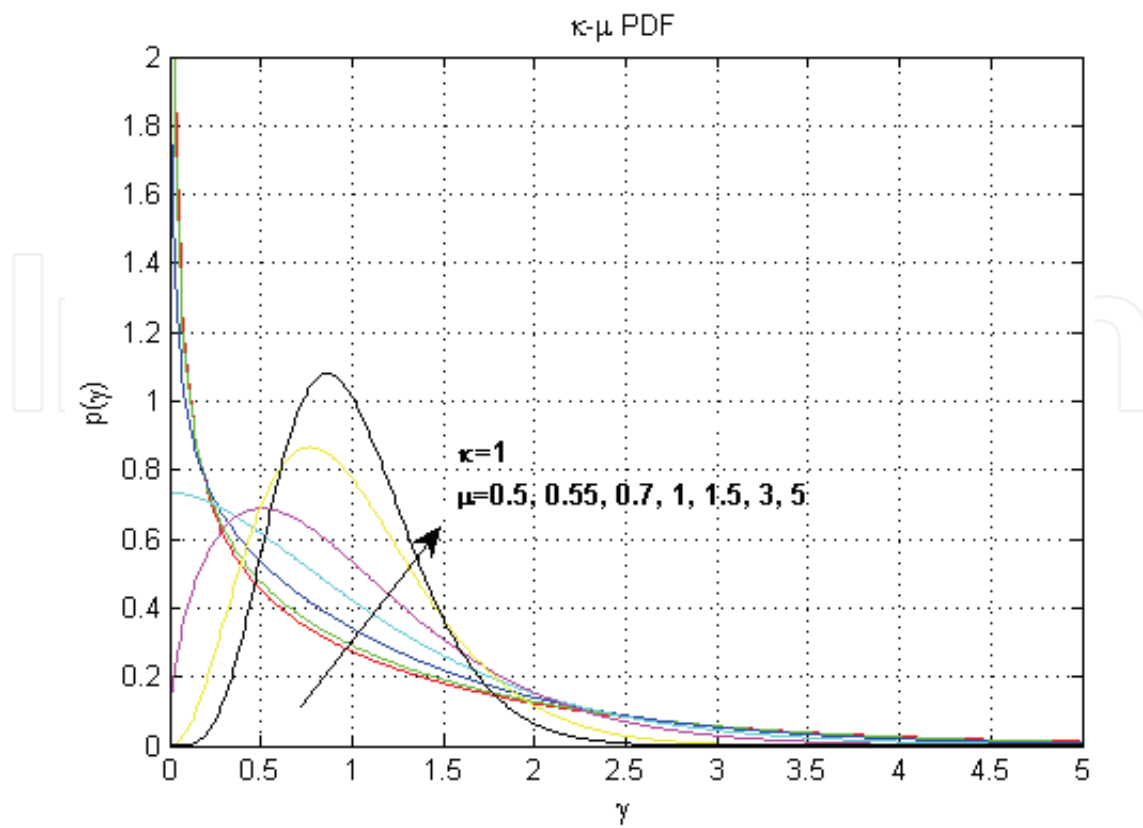


Fig. 1. PDF of SNR for $\kappa=1$ and various values of μ

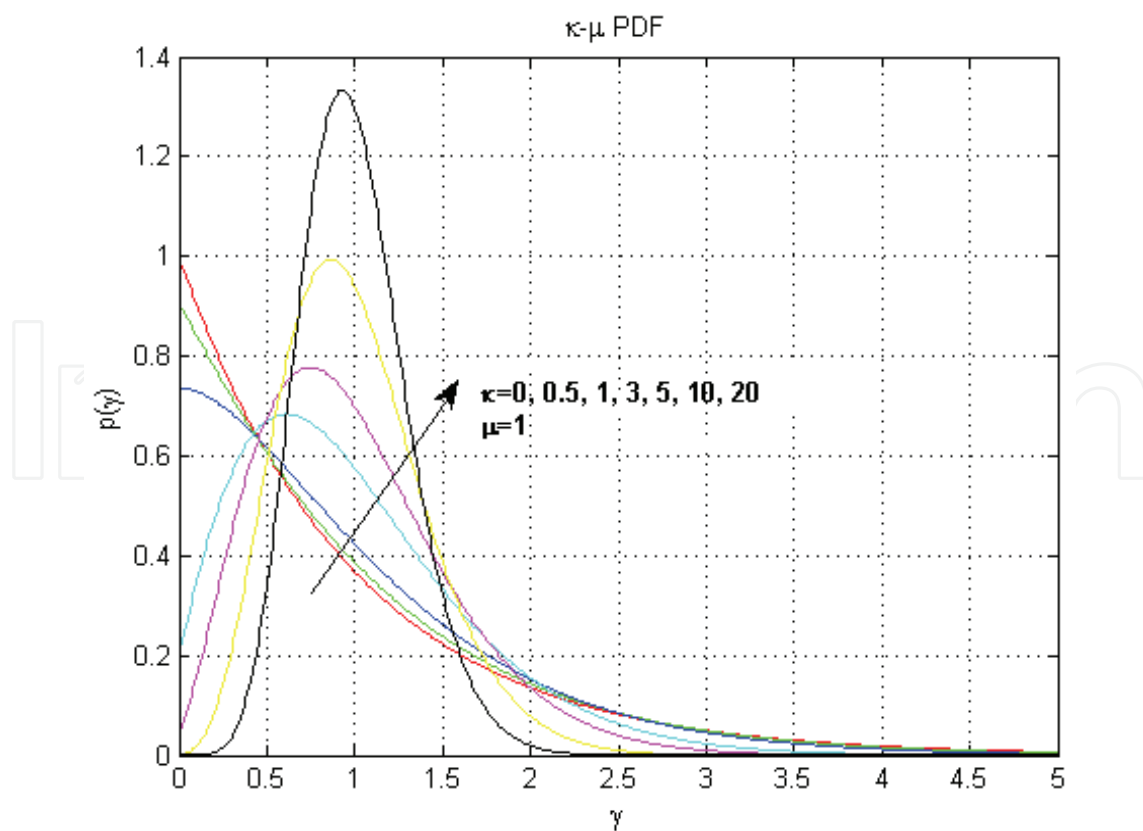


Fig. 2. PDF of SNR for $\mu=1$ and various values of κ

2.2 The η - μ distribution

The η - μ distribution is a general fading distribution that can be used to better represent the small-scale variations of the fading signal in a No-Line-of-Sight (NLoS) conditions. The fading model for the η - μ distribution considers a signal composed of clusters of multipath waves, propagating in a nonhomogenous environment. Within single cluster, the phases of the scattered waves are random and have similar delay times, with delay-time spreads of different clusters being relatively large. The in-phase and quadrature components of the fading signal within each cluster are assumed to be independent from each other, and to have different powers. Envelope R , and instantaneous power P_R can be written in terms of the in-phase and quadrature components of the fading signal as:

$$R^2 = P_R = \sum_{i=1}^n (X_i^2 + Y_i^2) \quad (12)$$

, where X_i and Y_i are mutually independent Gaussian processes with $\overline{X_i} = \overline{Y_i} = 0$, $\overline{X_i^2} = \sigma_X^2$, $\overline{Y_i^2} = \sigma_Y^2$, and n is the number of clusters of multipath. Total power of the i -th cluster is $P_{R,i} = R_i^2 = X_i^2 + Y_i^2$. Since $P_{R,i}$ equals to the sum of two central Gaussian RVs with non-identical variances, its MGF yields in:

$$M_{P_{R,i}}(s) = \frac{\sqrt{h}}{(1+\eta^{-1})\sigma_X^2} \frac{1}{\sqrt{\left(s - \frac{h}{(1+\eta^{-1})\sigma_X^2}\right)^2 - \left(\frac{H}{(1+\eta^{-1})\sigma_X^2}\right)^2}} \quad (13)$$

, where $\eta = \frac{\sigma_X^2}{\sigma_Y^2}$ is the scattered-wave power ratio between the in-phase and quadrature components of each cluster of multipath, $h = \frac{2+\eta^{-1}+\eta}{4}$, $H = \frac{\eta^{-1}-\eta}{4}$. Following the same procedure as in the case of κ - μ distribution, the MGF of the $f_{P_R}(P_R)$, where $P_R = \sum_{i=1}^n P_{R,i}$, is found to be:

$$M_{P_R}(s) = \prod_{i=1}^n M_{P_{R,i}}(s) = \left[\frac{\sqrt{h}}{(1+\eta^{-1})\sigma_X^2} \frac{1}{\sqrt{\left(s + \frac{h}{(1+\eta^{-1})\sigma_X^2}\right)^2 - \left(\frac{H}{(1+\eta^{-1})\sigma_X^2}\right)^2}} \right]^n \quad (14)$$

The inverse of (14) is given by (Abramowitz and Stegun, 1972, eq. 29.3.60):

$$f_{P_R}(P_R) = \frac{\sqrt{\pi n} \frac{n+1}{2} h^{\frac{n}{2}}}{(2H)^{\frac{n-1}{2}} \Gamma\left(\frac{n}{2}\right)} \cdot \frac{(P_R)^{\frac{n-1}{2}}}{\left(n(1+\eta^{-1})\sigma_X^2\right)^{\frac{n+1}{2}}} \cdot \exp\left(-\frac{h \cdot P_R}{(1+\eta^{-1})\sigma_X^2}\right) \cdot I_{\frac{n-1}{2}}\left(\frac{H \cdot P_R}{(1+\eta^{-1})\sigma_X^2}\right) \quad (15)$$

, where $I_n(\cdot)$ stands for n -th order modified Bessel function of the first kind. It can be seen that $\Omega = R^2 = \overline{P}_R = n(1 + \eta^{-1})\sigma_X^2 = n(1 + \eta)\sigma_Y^2$, and $\overline{R^4} = \overline{P_R^2} = [2n(1 + \eta^2) + n^2(1 + \eta^2)] \cdot \sigma_Y^4$. Thus,

$$\frac{(\overline{R^2})^2}{\overline{R^4} - (\overline{R^2})^2} = \frac{(\overline{P_R})^2}{\overline{P_R^2} - (\overline{P_R})^2} = \frac{n}{2} \cdot \frac{(1 + \eta)^2}{(1 + \eta^2)} \quad (16)$$

From (16), note that $n/2$ may be expressed in terms of physical parameters, such as mean-squared value of the power, the variance of the power, and the ratio of the total power of the dominant components and the total power of the scattered waves. Note also, that whereas these physical parameters are of a continuous nature, $n/2$ is of a discrete nature (integer multiple of $1/2$). It is plausible to presume that if these parameters are to be obtained by field measurements, their ratios, as defined in (16), will certainly lead to figures that may depart from the exact $n/2$. Several reasons exist for this. One of them, and probably the most meaningful, is that although the model proposed here is general, it is in fact an approximate solution to the so-called random phase problem, as are all the other well-known fading models approximate solutions to the random phase problem. The limitation of the model can be made less stringent by defining μ to be:

$$\mu = \frac{(\overline{R^2})^2}{\overline{R^4} - (\overline{R^2})^2} \cdot \frac{(1 + \eta^2)}{(1 + \eta)^2} = \frac{(\overline{P_R})^2}{\overline{P_R^2} - (\overline{P_R})^2} \cdot \frac{(1 + \eta^2)}{(1 + \eta)^2} = \frac{(\overline{P_R})^2}{2 \cdot (\overline{P_R^2} - (\overline{P_R})^2)} \cdot \left(1 + \left(\frac{H}{h}\right)^2\right) \quad (17)$$

, with μ being the real extension of $\frac{n}{2}$. Values of μ that differ from $\frac{n}{2}$ may account for:

- non-Gaussian nature of the in-phase and quadrature components of each cluster of the fading signal,
- non-zero correlation among the clusters of multipath components,
- non-zero correlation between in-phase and quadrature components within each cluster, etc.

So, the same analysis conducted for κ - μ applies to η - μ as well. Using the definitions for parameters η and μ , and the considerations as given above, the η - μ power PDF can be written from (15) as:

$$f_{P_R}(P_R) = \frac{2\sqrt{\pi} \cdot \mu^{\mu+0.5} \cdot h^\mu}{\Gamma(\mu) \cdot H^{\mu-0.5} \cdot \Omega^{\mu+0.5}} \cdot P_R^{\mu-0.5} \cdot \exp\left(-\frac{2\mu h \cdot P_R}{\Omega}\right) \cdot I_{\mu-0.5}\left(\frac{2\mu H \cdot P_R}{\Omega}\right) \quad (18)$$

Therefore, the η - μ envelope PDF can be obtained from (18) as:

$$f_R(R) = \frac{4\sqrt{\pi} \cdot \mu^{\mu+0.5} \cdot R^{2\mu}}{\Gamma(\mu) \cdot H^{\mu-0.5} \cdot \Omega^{\mu+0.5}} \cdot \exp\left[-\frac{2\mu h \cdot R^2}{\Omega}\right] \cdot I_{\mu-0.5}\left[\frac{2\mu H \cdot R^2}{\Omega}\right] \quad (19)$$

Instantaneous and average SNR are given by: $\gamma = \frac{P_R}{N_0} = \frac{R^2}{N_0}$, $\overline{\gamma} = \frac{\overline{P_R}}{N_0} = \frac{\Omega}{N_0}$, and therefore the η - μ SNR PDF can be obtained from (18) as:

$$f_{\gamma}(\gamma) = \frac{2\sqrt{\pi} \cdot \mu^{\mu+0.5} \cdot h^{\mu} \cdot \gamma^{\mu-0.5}}{\Gamma(\mu) \cdot H^{\mu-0.5} \cdot (\bar{\gamma})^{\mu+0.5}} \cdot \exp\left(-\frac{2\mu \cdot h \cdot \gamma}{\bar{\gamma}}\right) \cdot I_{\mu-0.5}\left(\frac{2\mu \cdot H \cdot \gamma}{\bar{\gamma}}\right) \quad (20)$$

From (20) we can derive CDF of instantaneous SNR as:

$$F_{\gamma}(\gamma) = \int_0^{\gamma} f_{\gamma}(t) dt = 1 - \Theta_{\mu} \left[\frac{H}{h}, \sqrt{\frac{2h\mu \cdot \gamma}{\bar{\gamma}}} \right] \quad (21)$$

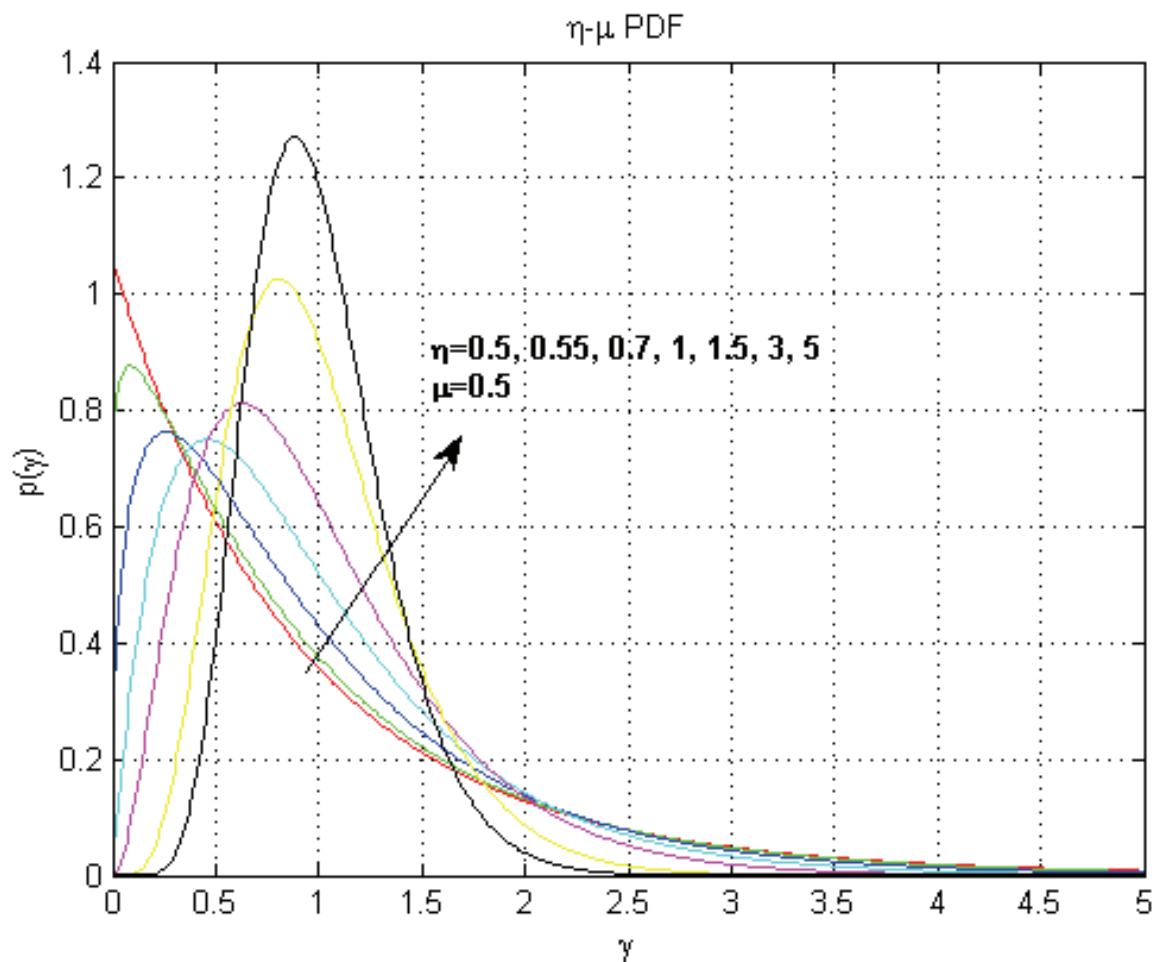


Fig. 3. PDF of SNR for $\mu=0,5$ and various values of η

Since previous integral doesn't have closed-form solution, function Θ has been defined as:

$$\Theta_{\nu}(a,b) = \frac{2^{1,5-\nu} \cdot \sqrt{\pi} \cdot (1-a^2)^{\nu}}{a^{\nu-0,5} \cdot \Gamma(\nu)} \cdot \int_b^{\infty} t^{2\nu} \cdot \exp(-t^2) \cdot I_{\nu-0,5}(at^2) \cdot dt \quad (22)$$

Now we can obtain closed-form expression for the n -th order moment of RV γ as:

$$\bar{\gamma}^n = \frac{\Gamma(2\mu+n)}{\Gamma(2\mu) \cdot h^{\mu+n}} \cdot \left(\frac{\bar{\gamma}}{2\mu}\right)^n \cdot {}_2F_1\left(\mu+n+0,5, \mu+\frac{n}{2}; \mu+0,5; \left(\frac{H}{h}\right)^2\right) \quad (23)$$

, where ${}_2F_1(\cdot, \cdot; \cdot; \cdot)$ represents Gauss hypergeometric function (Abramowitz and Stegun, 1972, eq. 15.1.1). The κ - μ and the η - μ distributions are indeed general fading distributions, which can be seen by a following special cases:

- $\mu=0,5$ and $\kappa=0$, the κ - μ distribution becomes One-sided Gaussian distribution;
- $\mu=0,5$ and $\eta=0$ (or $\eta \rightarrow \infty$), the η - μ distribution becomes One-sided Gaussian distribution;
- $\mu=1$ and $\kappa=0$, the κ - μ distribution becomes Rayleigh distribution;
- $\mu=0,5$ and $\eta=1$, the η - μ distribution becomes Rayleigh distribution;
- $\mu=1$ and $\kappa=K$, the κ - μ distribution becomes Rice distribution, where K represents Rice K parameter;
- $\mu=0,5$ and $\eta=q^2$, the η - μ distribution becomes Hoyt (Nakagami- q) distribution, where q represents Hoyt q parameter;
- $\mu=m$ and $\kappa=0$, the κ - μ distribution becomes Nakagami- m distribution, where m represents Nakagami m parameter;
- $\mu=m$ and $\eta=0$ (or $\eta \rightarrow \infty$), or $\mu=m/2$ and $\eta=1$, the η - μ distribution becomes Nakagami- m distribution, where m represents Nakagami m parameter.

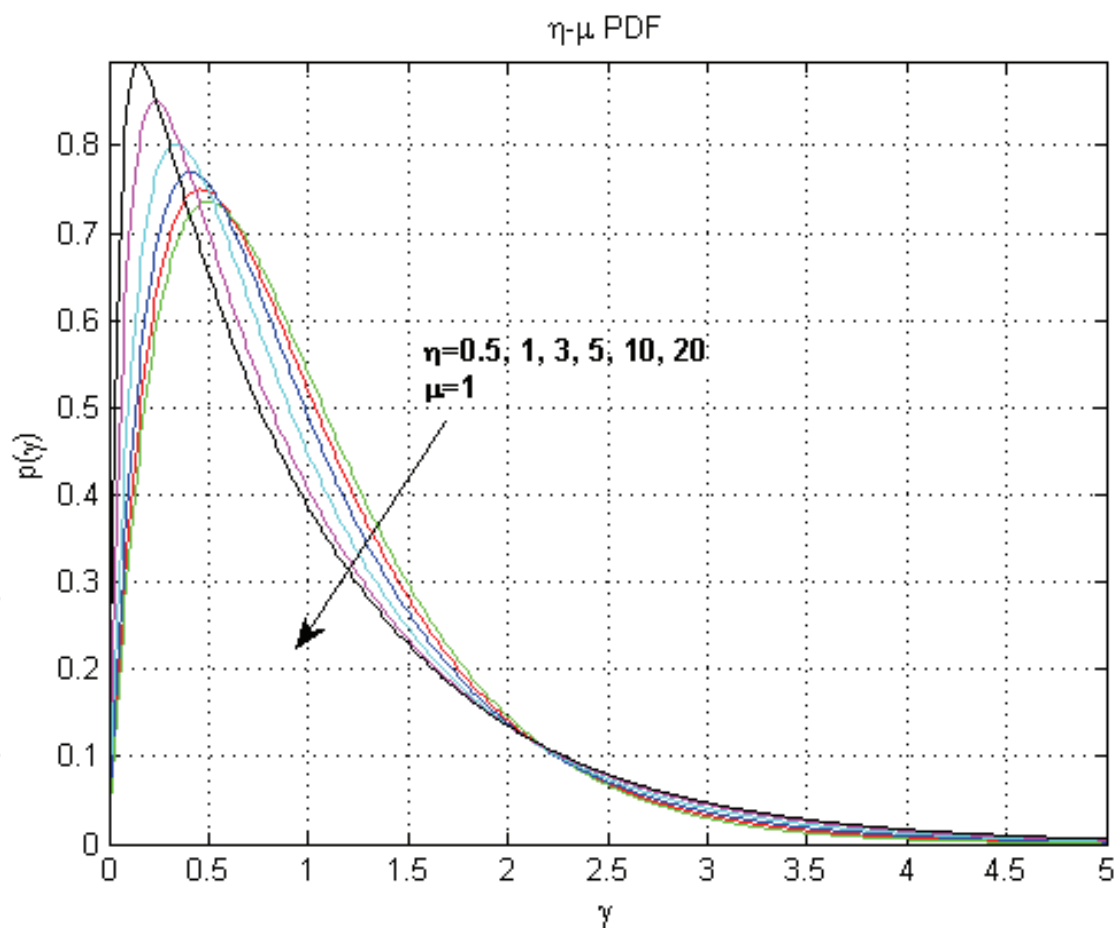


Fig. 4. PDF of SNR for $\eta=0,5$ and various values of μ

3. Maximal-ratio combining

There are four principal types of combining techniques (Simon & Alouini, 2005.) that depend essentially on the complexity restrictions put on the communication system and

amount of channel state information (CSI) available at the receiver. As shown in (Simon & Alouini, 2005.), in the absence of interference, Maximal-Ratio Combining is the optimal combining scheme, regardless of fading statistics, but most complex since MRC requires knowledge of all channel fading parameters (amplitudes, phases and time delays). Since knowledge of channel fading amplitudes is needed for MRC, this scheme can be used in conjunction with unequal energy signals, such as M-QAM or any other amplitude/phase modulations. In this paper we will treat L-branch MRC receiver. As shown in (Simon & Alouini, 2005.) MRC receiver is the optimal multichannel receiver, regardless of fading statistics in various diversity branches since it results in a ML receiver. For equiprobable transmitted symbols, the total SNR per symbol at the output of the MRC is given by (Stuber, 1996.): $\gamma = \sum_{j=1}^L \gamma_j$, where γ_j is instantaneous SNR in j -th branch of L-branch MRC receiver.

3.1 Maximal-ratio combining in presence of κ - μ distributed fading

We will first analyze statistics of received power and SNR at MRC output in presence of κ - μ distributed fading, and then we will obtain expression for outage probability at MRC output. Repeating the same procedure as in the previous section, previous relation can be written as:

$$\gamma = \sum_{j=1}^L \gamma_j = \frac{1}{N_0} \cdot \sum_{j=1}^L P_{R,j} = \frac{1}{N_0} \cdot \sum_{j=1}^L \sum_{i=1}^n P_{R,j,i} \quad (24)$$

, where $P_{R,j,i}$ represents total received power of the i -th cluster manifested in the j -th branch of the MRC receiver. Using (1) one can obtain:

$$P_R = \sum_{j=1}^L \sum_{i=1}^n (X_{i,j} + p_{i,j})^2 + (Y_{i,j} + q_{i,j})^2. \quad (25)$$

Repeating the same procedure as in the previous section, one can obtain MGF of the RV P_R :

$$M_{P_R}(s) = \prod_{j=1}^L M_{P_{R,j}}(s) = \frac{\exp\left(\frac{sd^2}{1-2s\sigma^2}\right)}{(1-2s\sigma^2)^{L \cdot n}} \quad (26)$$

, where $d^2 = \sum_{j=1}^L d_j^2$. Inverse of (26) yields in PDF of the RV P_R :

$$f_{P_R}(P_R) = \frac{L\mu(1+\kappa)^{\frac{L\mu+1}{2}}}{\kappa^{\frac{L\mu-1}{2}} \cdot \exp(L\mu\kappa) \cdot (L \cdot \Omega)^{\frac{L\mu+1}{2}}} \cdot P_R^{\frac{L\mu-1}{2}} \cdot \exp\left[-\frac{\mu(1+\kappa) \cdot P_R}{\Omega}\right] \cdot I_{L\mu-1}\left[2\mu\sqrt{L\frac{\kappa(1+\kappa) \cdot P_R}{\Omega}}\right] \quad (27)$$

From PDF of received signal power at MRC output, we can obtain PDF of instantaneous SNR at MRC output:

$$f_{\gamma}(\gamma) = \frac{L\mu(1+\kappa)^{\frac{L\mu+1}{2}}}{\kappa^2 \cdot \exp(L\mu\kappa) \cdot (L \cdot \bar{\gamma})^{\frac{L\mu+1}{2}}} \cdot \gamma^{\frac{L\mu-1}{2}} \cdot \exp\left[-\frac{\mu(1+\kappa) \cdot \gamma}{\bar{\gamma}}\right] \cdot I_{L\mu-1}\left[2\mu\sqrt{L \frac{\kappa(1+\kappa) \cdot \gamma}{\bar{\gamma}}}\right] \quad (28)$$

Note that sum of L squares of the κ - μ distributed RVs is a square of κ - μ distributed RV, but with different parameters, which means SNR at the output of the MRC receiver subdue to the κ - μ distribution with parameters:

$$\mu_{MRC} = L \cdot \mu, \kappa_{MRC} = \kappa, \bar{\gamma}_{MRC} = L \cdot \bar{\gamma}.$$

Now, it is easy to obtain CDF of SNR at MRC output:

$$F_{\gamma}(\gamma) = \int_0^{\gamma} f_{\gamma}(t) \cdot dt = 1 - Q_{L\mu}\left[\sqrt{2L\kappa\mu}, \sqrt{\frac{2(\kappa+1)\mu \cdot \gamma}{\bar{\gamma}}}\right] \quad (29)$$

For fixed SNR threshold γ_{th} , outage probability at MRC output is given by:

$$P_{out}(\gamma_{th}) = F_{\gamma}(\gamma_{th}) = \int_0^{\gamma_{th}} f_{\gamma}(t) \cdot dt = 1 - Q_{L\mu}\left[\sqrt{2L\kappa\mu}, \sqrt{\frac{2(\kappa+1)\mu \cdot \gamma_{th}}{\bar{\gamma}}}\right] \quad (30)$$

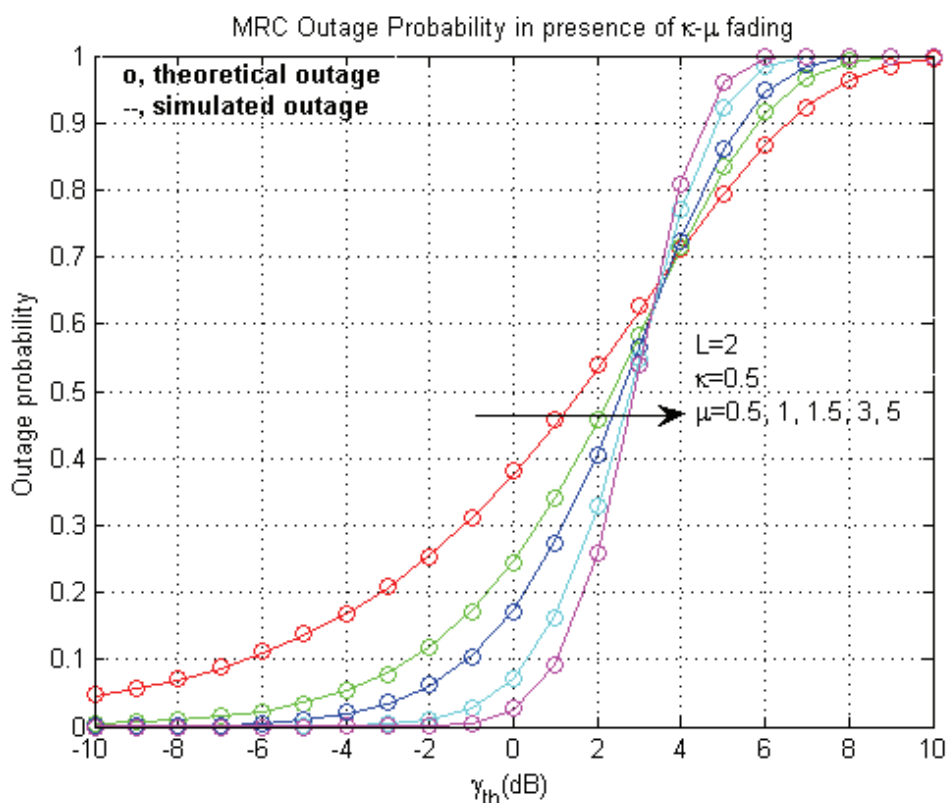


Fig. 5. Outage probability for dual-branch MRC ($L=2$), fixed κ , and various μ

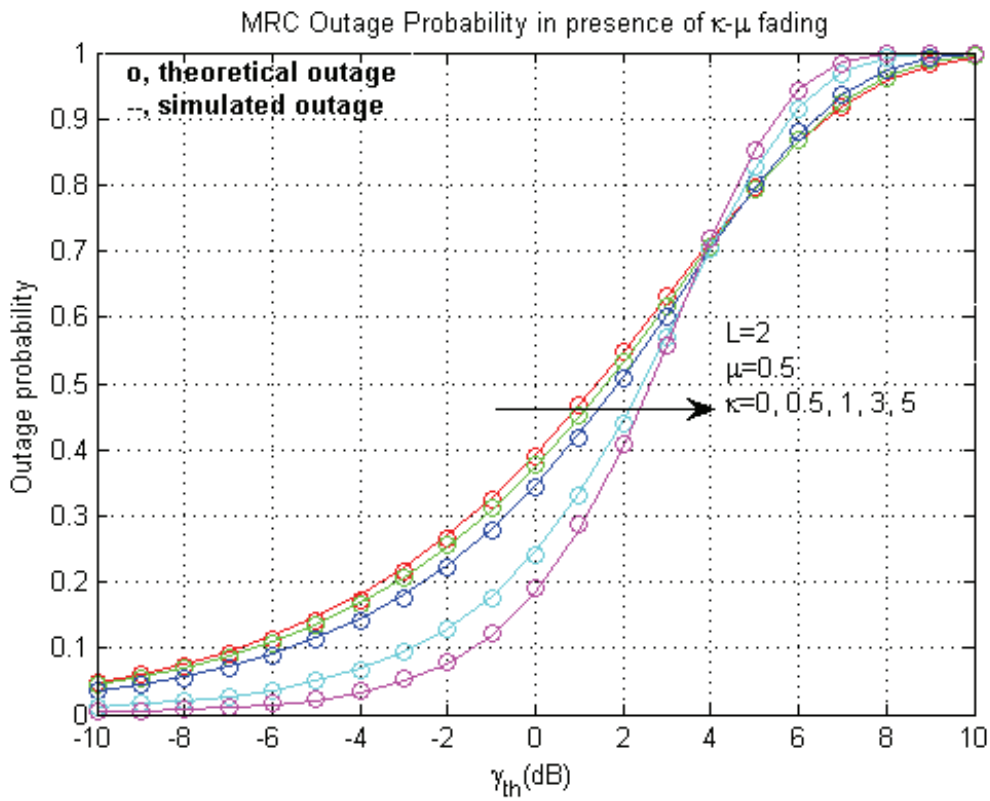


Fig. 6. Outage probability for dual-branch MRC ($L=2$), fixed μ , and various κ

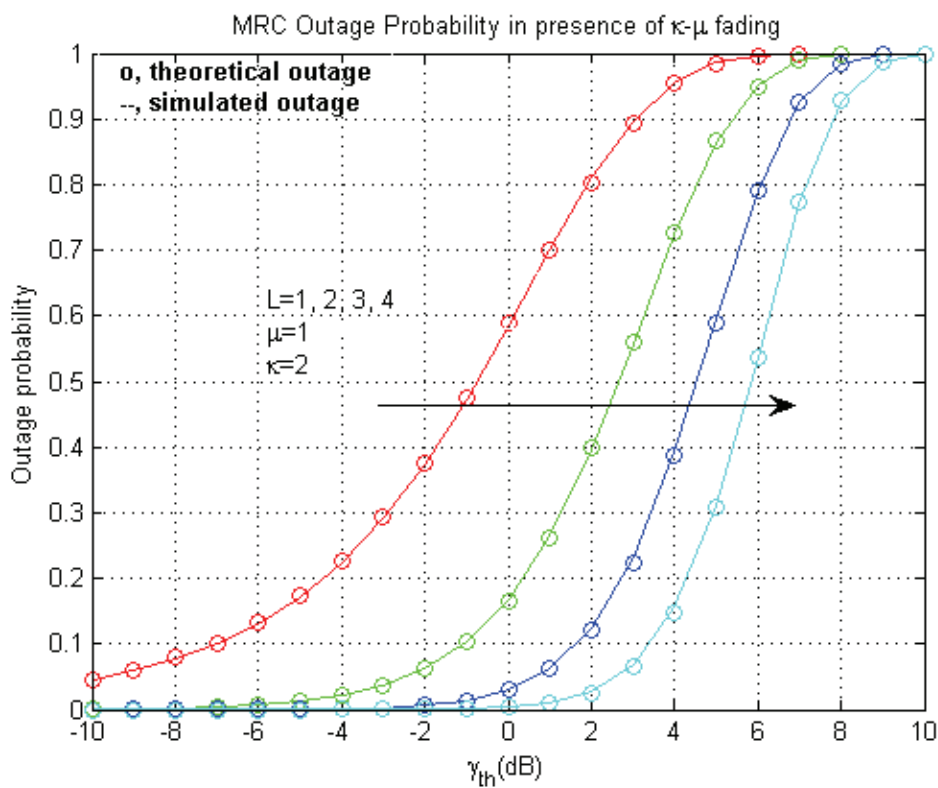


Fig. 7. Outage probability for fixed μ and κ , $L=1, 2, 3$ and 4

3.2 Maximal-ratio combining in presence of η - μ distributed fading

Now we analyze statistics of received power and SNR at MRC output in presence of η - μ distributed fading, and after that, we will obtain expression for outage probability at MRC output. Using (12) one can obtain:

$$P_R = \sum_{j=1}^L \sum_{i=1}^n (X_{i,j}^2 + Y_{i,j}^2) \quad (31)$$

Repeating the same procedure as in the previous section one can obtain MGF of the RV P_R :

$$M_{P_R}(s) = \prod_{j=1}^L M_{P_{R,j}}(s) = \left[\frac{\sqrt{h}}{(1 + \eta^{-1})\sigma_X^2} \right]^{L \cdot n} \frac{1}{\sqrt{\left(s + \frac{h}{(1 + \eta^{-1})\sigma_X^2} \right)^2 - \left(\frac{H}{(1 + \eta^{-1})\sigma_X^2} \right)^2}} \quad (32)$$

Inverse of Equation (32) yields to PDF of the RV P_R :

$$f_{P_R}(P_R) = \frac{2\sqrt{\pi} \cdot \mu^{L \cdot \mu + 0.5} \cdot h^{L \cdot \mu}}{\Gamma(L \cdot \mu) \cdot H^{L \cdot \mu - 0.5} \cdot \Omega^{L \cdot \mu + 0.5}} \cdot P_R^{L \cdot \mu - 0.5} \cdot \exp\left(-\frac{2\mu h \cdot P_R}{\Omega}\right) \cdot I_{L \cdot \mu - 0.5}\left(\frac{2\mu H \cdot P_R}{\Omega}\right) \quad (33)$$

From PDF of received signal power at MRC output, we can obtain PDF of instantaneous SNR at MRC output:

$$f_\gamma(\gamma) = \frac{2\sqrt{\pi} \cdot \mu^{L \cdot \mu + 0.5} \cdot h^{L \cdot \mu}}{\Gamma(L \cdot \mu) \cdot H^{L \cdot \mu - 0.5} \cdot (\bar{\gamma})^{L \cdot \mu + 0.5}} \cdot \gamma^{L \cdot \mu - 0.5} \cdot \exp\left(-\frac{2\mu h \cdot \gamma}{\bar{\gamma}}\right) \cdot I_{L \cdot \mu - 0.5}\left(\frac{2\mu H \cdot \gamma}{\bar{\gamma}}\right) \quad (34)$$

Note that sum of L squares of the η - μ distributed RVs is a square of η - μ distributed RV, but with different parameters, which means SNR at the output of the MRC receiver subdue to the η - μ distribution with parameters:

$$\mu_{MRC} = L \cdot \mu, \eta_{MRC} = \eta, \bar{\gamma}_{MRC} = L \cdot \bar{\gamma}.$$

Now, CDF of instantaneous SNR at MRC output is given by:

$$F_\gamma(\gamma) = \int_0^\gamma f_\gamma(t) \cdot dt = 1 - \Theta_{L\mu} \left[\frac{H}{h}, \sqrt{\frac{2h\mu \cdot \gamma}{\bar{\gamma}}} \right] \quad (35)$$

, where Θ is defined in (22). For fixed SNR threshold γ_{th} , outage probability at MRC output is given by:

$$P_{out}(\gamma_{th}) = F_\gamma(\gamma_{th}) = \int_0^{\gamma_{th}} f_\gamma(t) \cdot dt = 1 - \Theta_{L\mu} \left[\frac{H}{h}, \sqrt{\frac{2h\mu \cdot \gamma_{th}}{\bar{\gamma}}} \right] \quad (36)$$

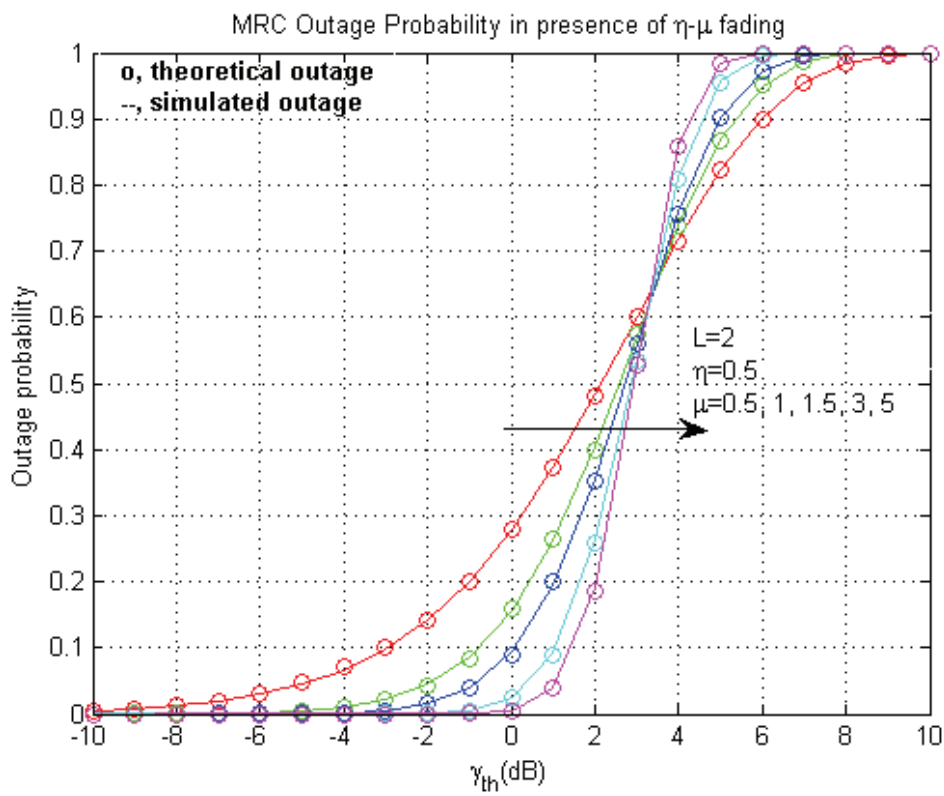


Fig. 8. Outage probability for dual-branch MRC (L=2), fixed η , and various μ

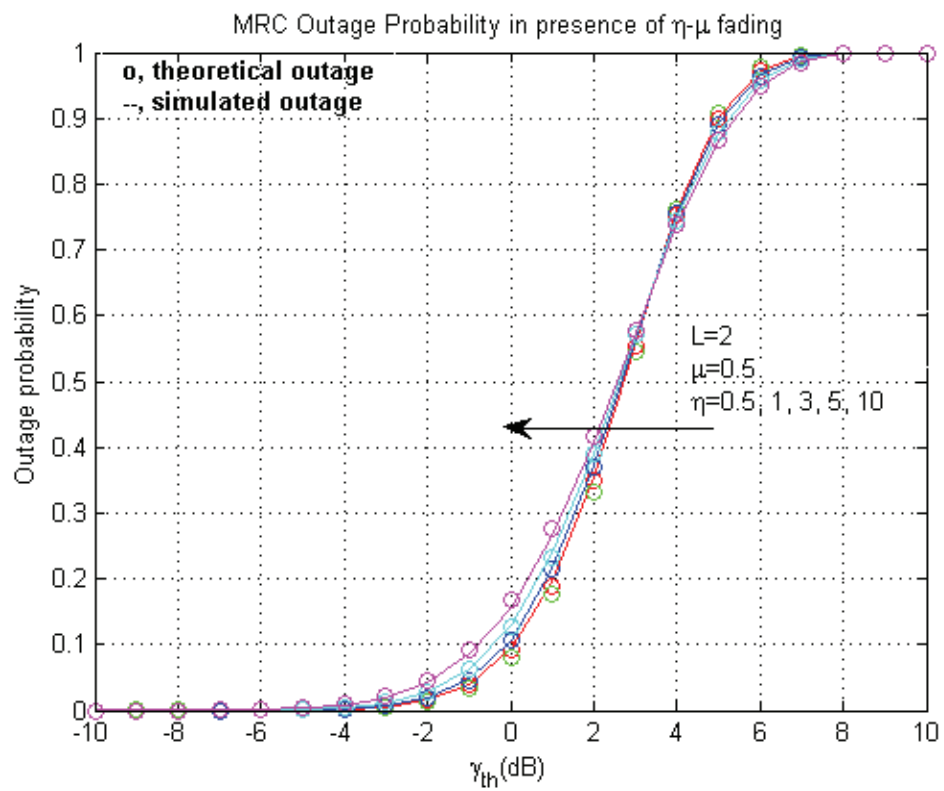


Fig. 9. Outage probability for dual-branch MRC (L=2), fixed μ , and various η

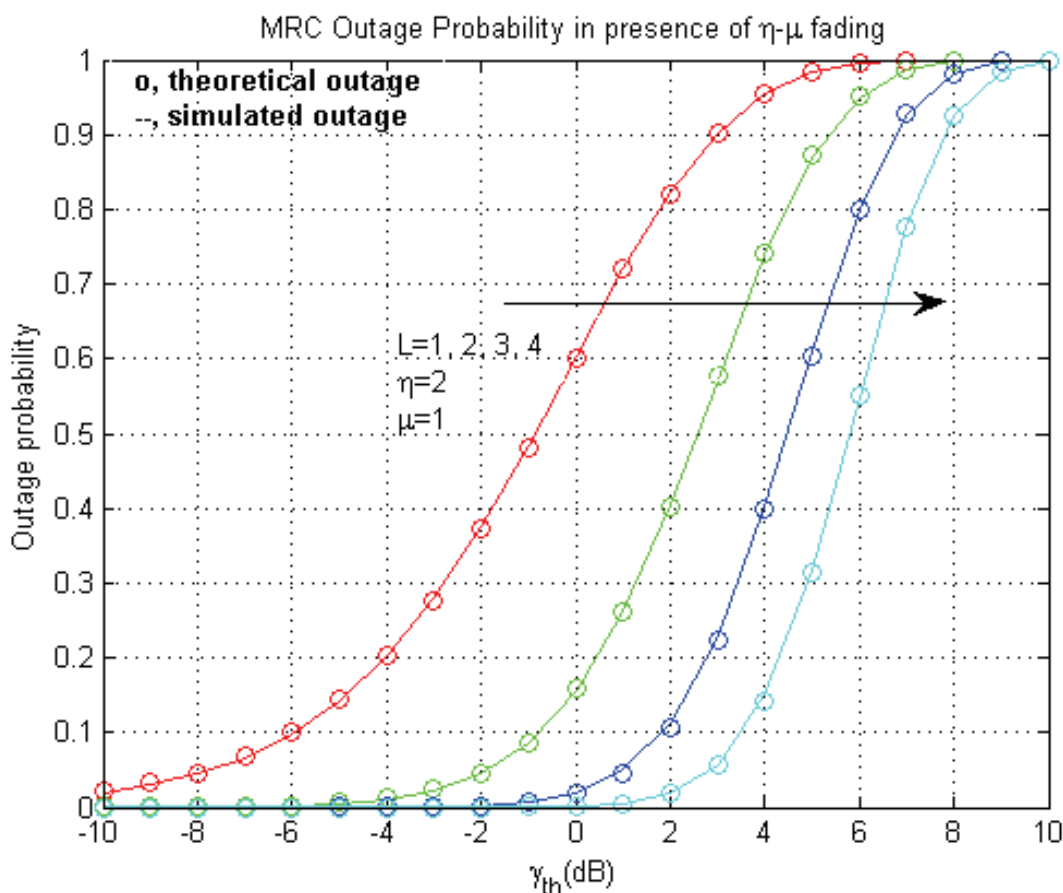


Fig. 10. Outage probability for fixed μ and η , $L=1, 2, 3$ and 4

4. Symbol error probability analysis

When we analyze symbol error probability (SEP), we must focus upon single modulation format because different modulations result in different SEPs. We must also consider type of detection (coherent or non-coherent). Namely, decision-block of coherent receiver performs decision based upon information gained in both In-phase and quadrature components, while decision-block of non-coherent receiver performs decision based only upon envelope of the received signal. Although coherent detection results in smaller SEP than corresponding non-coherent detection for the same SNR, sometimes it is suitable to perform non-coherent detection depending on receiver structure complexity.

Non-coherent detection

To obtain average SEP for non-coherent detection, we will use generic expression for instantaneous SEP: $SEP = a \cdot \exp(-b \cdot \gamma)$, where γ represents instantaneous received SNR, and non-negative parameters a and b depend on used modulation format.

Average SEP can be obtained by averaging expression for SEP with respect to γ :

$$ASEP = \int_0^{+\infty} SEP \cdot f_\gamma(\gamma) \cdot d\gamma = \int_0^{+\infty} a \cdot \exp(-b \cdot \gamma) \cdot f_\gamma(\gamma) \cdot d\gamma \quad (38)$$

	b	0.5	1
a			
0.5		BFSK	DBPSK
1		/	/
$\frac{M-1}{2}$		MFSK	/

Table 1. Values of a and b for some non-coherent modulations**Coherent detection**

To obtain average SEP for coherent detection, we will use generic expression for instantaneous SEP: $SEP = a \cdot Q(\sqrt{b \cdot \gamma})$, where $Q(\bullet)$ function is defined as:

$$Q(x) = \frac{1}{\sqrt{2\pi}} \int_x^{+\infty} \exp\left(-\frac{t^2}{2}\right) \cdot dt$$

, and non-negative parameters a and b depend on used modulation format.

	b	1	2	$2 \sin^2\left(\frac{\pi}{M}\right)$	$\frac{3}{M-1}$
a					
1		BFSK	BPSK	/	/
2		QPSK	DBPSK	MPSK	/
$4 \frac{\sqrt{M}-1}{\sqrt{M}}$		/	/	/	Rect. QAM

Table 2. Values of a and b for some coherent modulations

Average SEP can be obtained by averaging expression for SEP with respect to γ :

$$ASEP = \int_0^{+\infty} SEP \cdot f_\gamma(\gamma) \cdot d\gamma = \int_0^{+\infty} a \cdot Q(\sqrt{b \cdot \gamma}) \cdot f_\gamma(\gamma) \cdot d\gamma \quad (39)$$

Nevertheless, it is sometimes impossible to find closed-form solution for (11). Because of that, we will present exact MGF-based solution, and solutions based on lower and upper bound of the Q function. To obtain MGF-based solution, first we have to rewrite Q function in more suitable form as in (Simon & Alouini, 2005.):

$$Q(x) = \frac{1}{\pi} \cdot \int_0^{\frac{\pi}{2}} \exp\left(\frac{-x^2}{2 \sin^2 \theta}\right) \cdot d\theta$$

Introducing alternate form of Q function in to the ASEP expression, we obtain MGF-based solution:

$$\begin{aligned}
 ASEP &= a \cdot \int_0^{+\infty} Q(\sqrt{b \cdot \gamma}) \cdot f_\gamma(\gamma) \cdot d\gamma = \\
 &= \frac{a}{\pi} \cdot \int_0^{+\infty} \int_0^{\frac{\pi}{2}} \exp\left(\frac{-b \cdot \gamma}{2 \sin^2 \theta}\right) \cdot d\theta \cdot f_\gamma(\gamma) \cdot d\gamma \\
 ASEP &= \frac{a}{\pi} \cdot \int_0^{\frac{\pi}{2}} \left(\int_0^{+\infty} \exp\left(\frac{-b \cdot \gamma}{2 \sin^2 \theta}\right) \cdot f_\gamma(\gamma) \cdot d\gamma \right) \cdot d\theta = \frac{a}{\pi} \cdot \int_0^{\frac{\pi}{2}} M_\gamma\left(\frac{-b}{2 \sin^2 \theta}\right) \cdot d\theta \quad (40)
 \end{aligned}$$

Now we seek solutions based on upper and lower bound of Q function. Q function can be bounded as:

$$\frac{\exp\left(\frac{-x^2}{2}\right)}{x\sqrt{2\pi}} \cdot \left(1 - \frac{1}{x^2}\right) < Q(x) < \frac{\exp\left(\frac{-x^2}{2}\right)}{x\sqrt{2\pi}} \quad (41)$$

Upper bound for ASEP can be obtained by introducing upper bound of the Q function in (39):

$$ASEP_{UB} = \int_0^{+\infty} \frac{a}{\sqrt{2\pi b \cdot \gamma}} \cdot \exp\left(\frac{-b \cdot \gamma}{2}\right) \cdot f_\gamma(\gamma) \cdot d\gamma \quad (42)$$

Lower bound for ASEP can be obtained by introducing lower bound of the Q function in (39):

$$\begin{aligned}
 ASEP_{LB} &= \int_0^{+\infty} \frac{a}{\sqrt{2\pi b \cdot \gamma}} \cdot \left(1 - \frac{1}{b \cdot \gamma}\right) \cdot \exp\left(\frac{-b \cdot \gamma}{2}\right) \cdot f_\gamma(\gamma) \cdot d\gamma = \\
 &= ASEP_{UB} - \int_0^{+\infty} \frac{a}{\sqrt{2\pi (b \cdot \gamma)^3}} \cdot \exp\left(\frac{-b \cdot \gamma}{2}\right) \cdot f_\gamma(\gamma) \cdot d\gamma \quad (43)
 \end{aligned}$$

4.1 Symbol error probability analysis for maximal-ratio combiner in presence of κ - μ distributed fading

To obtain ASEP at MRC output for κ - μ fading for non-coherent detection, we introduce (28) in (38):

$$\begin{aligned}
 ASEP &= a \cdot \int_0^{+\infty} \exp(-b \cdot \gamma) \cdot f_\gamma(\gamma) \cdot d\gamma = \\
 &= a \cdot \frac{L\mu(1+\kappa)^{\frac{L\mu+1}{2}}}{\kappa^{\frac{L\mu-1}{2}} \cdot \exp(L\mu\kappa) \cdot (L \cdot \bar{\gamma})^{\frac{L\mu+1}{2}}} \cdot \int_0^{+\infty} \gamma^{\frac{L\mu-1}{2}} \cdot \exp\left[-\left(b + \frac{\mu(1+\kappa)}{\gamma}\right) \cdot \gamma\right] \cdot I_{L\mu-1}\left[2\mu\sqrt{L \frac{\kappa(1+\kappa) \cdot \gamma}{\bar{\gamma}}}\right] \cdot d\gamma
 \end{aligned}$$

Using (Prudnikov et al., 1992, eq. 5, page 318) we obtain closed-form expression for ASEP for non-coherent detection:

$$ASEP = a \cdot \left[\frac{\mu(1+\kappa)}{b \cdot \bar{\gamma} + \mu(1+\kappa)} \cdot \exp\left(\frac{-b\kappa \cdot \bar{\gamma}}{b \cdot \bar{\gamma} + \mu(1+\kappa)}\right) \right]^{L\mu} \quad (44)$$

Now we have to obtain ASEP at MRC output for κ - μ fading for coherent detection. To do so, first we have to manipulate (26) to obtain MGF for RV γ at MRC output:

$$M_\gamma(s) = \frac{\exp\left(\frac{\frac{L\kappa\bar{\gamma}}{1+\kappa} \cdot s}{1 - \frac{\bar{\gamma}}{\mu(1+\kappa)} \cdot s}\right)}{\left(1 - \frac{\bar{\gamma}}{\mu(1+\kappa)} \cdot s\right)^{L\mu}} \quad (45)$$

Introducing (45) in (40) we obtain:

$$ASEP = \frac{a}{\pi} \cdot \int_0^{\frac{\pi}{2}} M_\gamma\left(\frac{-b}{2\sin^2\theta}\right) \cdot d\theta = \frac{a}{\pi} \cdot \int_0^{\frac{\pi}{2}} \frac{\exp\left(\frac{\frac{L\kappa\bar{\gamma}}{1+\kappa} \cdot \frac{-b}{2\sin^2\theta}}{1 - \frac{\bar{\gamma}}{\mu(1+\kappa)} \cdot \frac{-b}{2\sin^2\theta}}\right)}{\left(1 - \frac{\bar{\gamma}}{\mu(1+\kappa)} \cdot \frac{-b}{2\sin^2\theta}\right)^{L\mu}} \cdot d\theta \quad (46)$$

Now we seek upper bound for ASEP for coherent detection by introducing (28) in (42):

$$\begin{aligned} ASEP_{UB} &= \int_0^{+\infty} \frac{a}{\sqrt{2\pi b \cdot \gamma}} \cdot \exp\left(\frac{-b \cdot \gamma}{2}\right) \cdot f_\gamma(\gamma) \cdot d\gamma = \\ &= \int_0^{+\infty} \frac{a}{\sqrt{2\pi b}} \cdot \frac{L\mu(1+\kappa)^{\frac{L\mu+1}{2}}}{\kappa^{\frac{L\mu-1}{2}} \cdot \exp(L\mu\kappa) \cdot (L \cdot \bar{\gamma})^{\frac{L\mu+1}{2}}} \cdot \\ &\quad \cdot \gamma^{\frac{L\mu-2}{2}} \exp\left[-\gamma\left(\frac{b}{2} + \frac{\mu(1+\kappa)}{\bar{\gamma}}\right)\right] \cdot I_{L\mu-1}\left[2\mu\sqrt{L \cdot \frac{\kappa(1+\kappa)\bar{\gamma}}{\gamma}}\right] \cdot d\gamma \end{aligned}$$

Using (Prudnikov et al., 1992, eq. 5, page 318) we obtain closed-form expression for upper bound for average SEP for coherent detection:

$$\begin{aligned} ASEP_{UB} &= \frac{a \cdot \Gamma(L\mu - 0.5)}{\sqrt{2\pi b} \cdot \Gamma(L\mu)} \cdot \left(\frac{\mu(1+\kappa)}{\exp(\kappa) \cdot \bar{\gamma}}\right)^{L\mu} \cdot \left(\frac{b}{2} + \frac{\mu(1+\kappa)}{\bar{\gamma}}\right)^{0.5-L\mu} \cdot \\ &\quad \cdot {}_1F_1\left(L\mu - 0.5; L\mu; \frac{\mu^2 L \kappa (1+\kappa)}{\frac{b \cdot \bar{\gamma}}{2} + \mu(1+\kappa)}\right) \end{aligned} \quad (47)$$

, where ${}_1F_1(\cdot; \cdot; \cdot)$ is Kummer confluent hypergeometric function defined in (Wolfram, <http://functions.wolfram.com/07.20.02.0001.01>). Lower bound for ASEP can be obtained by introducing (28) in (43), and using the same solution as in the previous case:

$$\begin{aligned}
 ASEP_{LB} = & \frac{a \cdot \Gamma(L\mu - 0.5)}{\sqrt{2\pi b} \cdot \Gamma(L\mu)} \cdot \left(\frac{\mu(1+\kappa)}{\exp(\kappa) \cdot \gamma} \right)^{L\mu} \cdot \left(\frac{b}{2} + \frac{\mu(1+\kappa)}{\gamma} \right)^{0.5-L\mu} \\
 & \cdot {}_1F_1 \left(L\mu - 0.5; L\mu; \frac{\mu^2 L \kappa (1+\kappa)}{\frac{b \cdot \gamma}{2} + \mu(1+\kappa)} \right) - \\
 & - \frac{a \cdot \Gamma(L\mu - 1.5)}{\sqrt{2\pi b^3} \cdot \Gamma(L\mu)} \cdot \left(\frac{\mu(1+\kappa)}{\exp(\kappa) \cdot \gamma} \right)^{L\mu} \cdot \left(\frac{b}{2} + \frac{\mu(1+\kappa)}{\gamma} \right)^{1.5-L\mu} \\
 & \cdot {}_1F_1 \left(L\mu - 1.5; L\mu; \frac{\mu^2 L \kappa (1+\kappa)}{\frac{b \cdot \gamma}{2} + \mu(1+\kappa)} \right)
 \end{aligned} \tag{48}$$

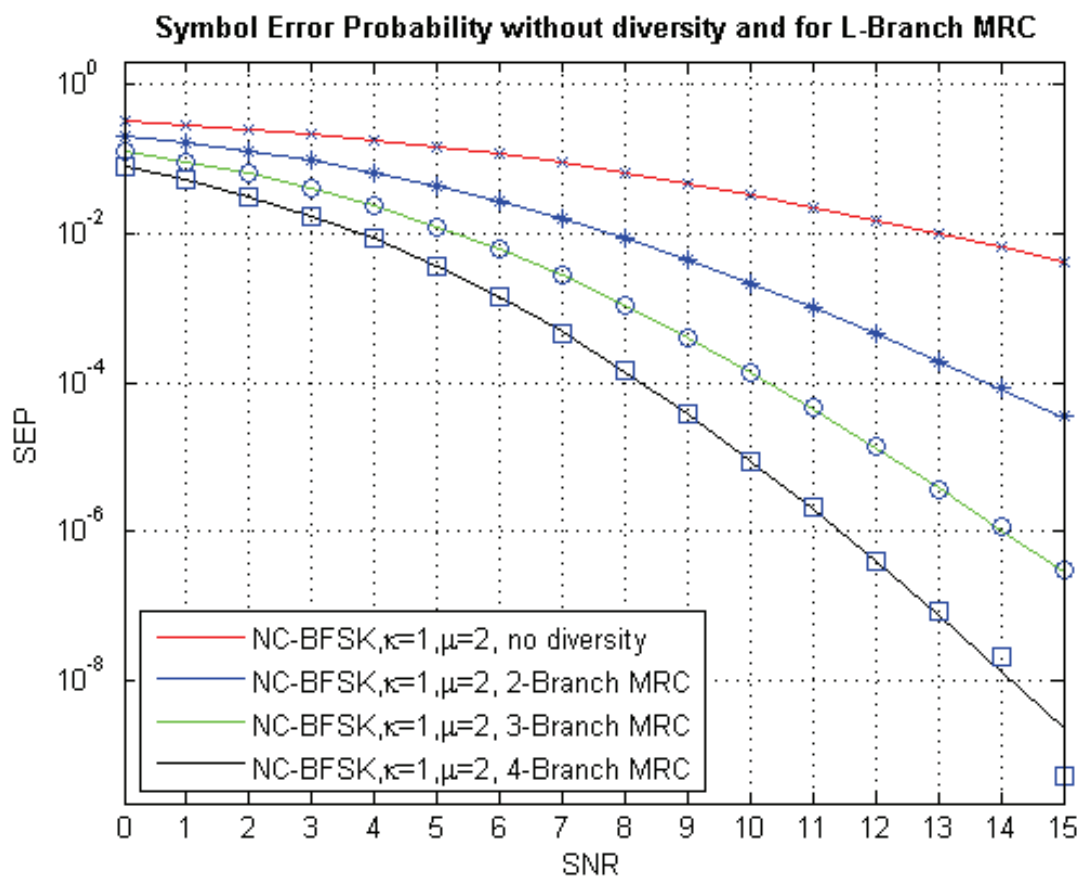


Fig. 11. Average symbol error probability for non-coherent BFSK, $L=1, 2, 3$ and 4

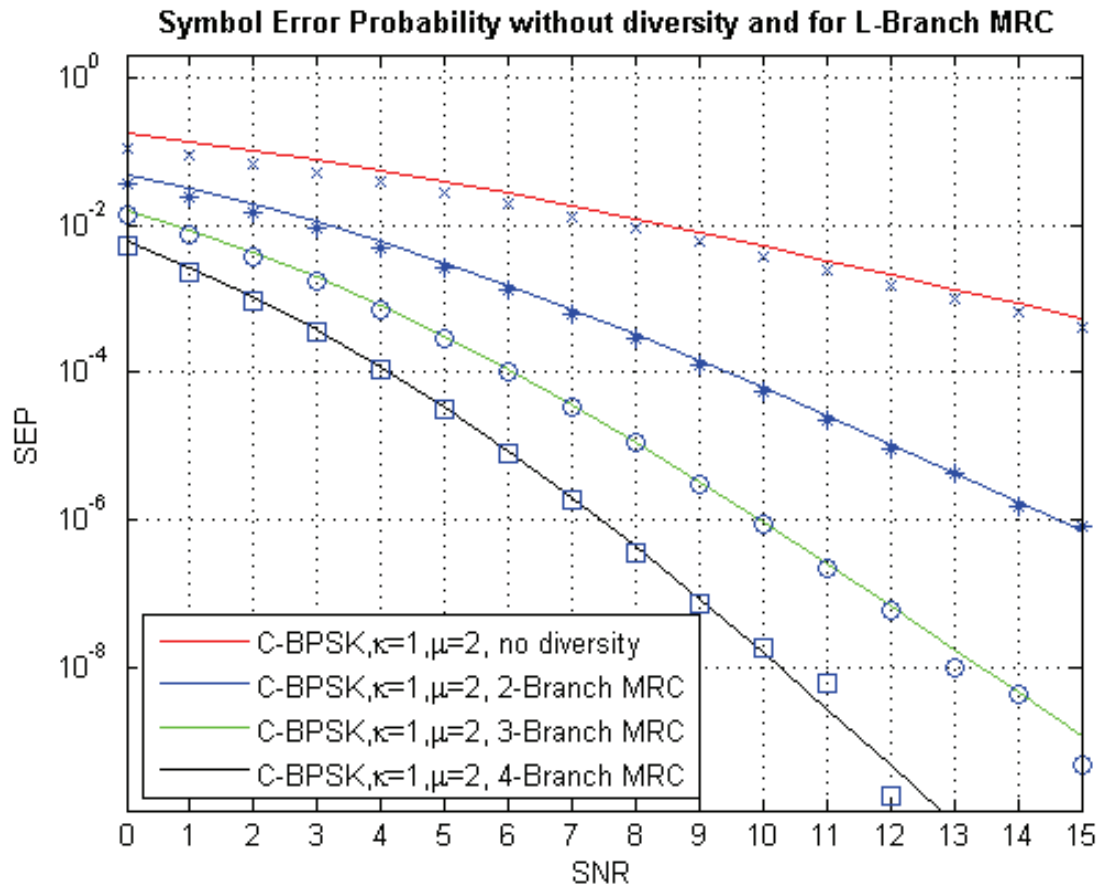


Fig. 12. Average symbol error probability for coherent BPSK, $L=1, 2, 3$ and 4

4.2 Symbol error probability analysis for maximal-ratio combiner in presence of η - μ distributed fading

To obtain ASEP at MRC output for η - μ fading for non-coherent detection, we introduce (34) in (38):

$$\begin{aligned}
 ASEP &= a \cdot \int_0^{+\infty} \exp(-b \cdot \gamma) \cdot f_{\gamma}(\gamma) \cdot d\gamma = \\
 &= a \cdot \frac{2\sqrt{\pi} \cdot \mu^{L \cdot \mu + 0.5} \cdot h^{L \cdot \mu}}{\Gamma(L \cdot \mu) \cdot H^{L \cdot \mu - 0.5} \cdot (\bar{\gamma})^{L \cdot \mu + 0.5}} \cdot \int_0^{+\infty} \gamma^{L \cdot \mu - 0.5} \cdot \exp\left[-\left(b + \frac{2\mu h}{\bar{\gamma}}\right) \cdot \gamma\right] \cdot I_{L \cdot \mu - 0.5}\left(\frac{2\mu H \cdot \gamma}{\bar{\gamma}}\right) \cdot d\gamma
 \end{aligned}$$

Integration of previous expression will be carried out via Meijer-G functions, defined in (Wolfram, <http://functions.wolfram.com/HypergeometricFunctions/MeijerG/>). First we have to transform exponential and Bessel functions in Meijer-G functions in accordance to (Wolfram, <http://functions.wolfram.com/07.34.03.0228.01>) and (Wolfram, <http://functions.wolfram.com/03.02.26.0009.01>). Integration is performed with (Wolfram, <http://functions.wolfram.com/07.34.21.0011.01>). After some algebraic manipulations, and simplifications in accordance to (Wolfram, <http://functions.wolfram.com/07.34.03.0734.01>)

and (Wolfram, <http://functions.wolfram.com/07.23.03.0079.01>), we obtain closed-form expression for average SEP for non-coherent detection:

$$ASEP = a \cdot \left[\frac{4\mu^2 h}{(b \cdot \bar{\gamma} + 2\mu h)^2 - (2\mu H)^2} \right]^{L\mu} \quad (49)$$

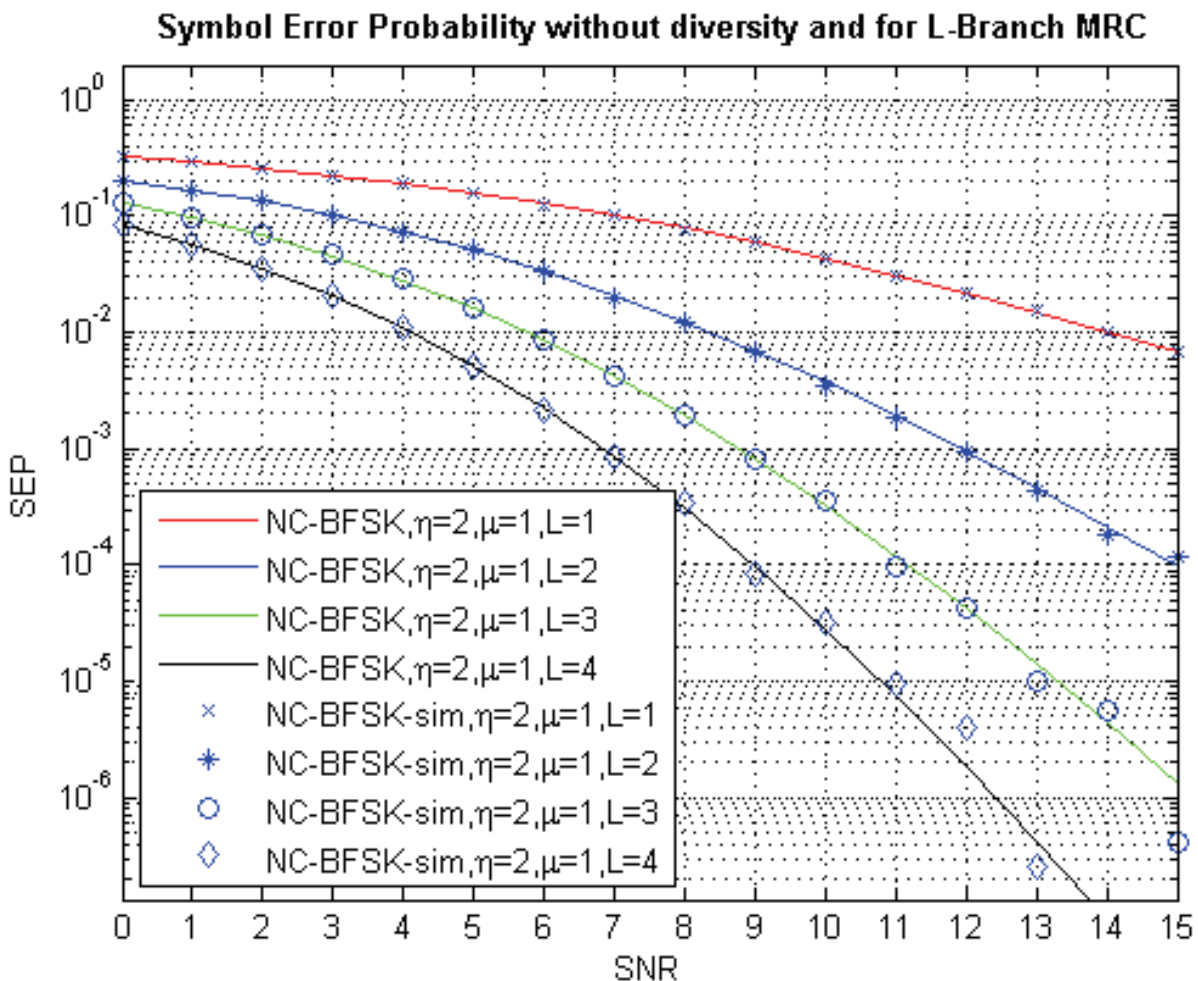


Fig. 13. Average symbol error probability for coherent BFSK, L=1, 2, 3 and 4

Now we have to obtain ASEP at MRC output for η - μ fading for coherent detection. First we manipulate (32) to obtain MGF for RV γ at MRC output:

$$M_{\gamma}(s) = \left[\frac{4\mu^2 h}{(s \cdot \bar{\gamma} - 2\mu h)^2 - (2\mu H)^2} \right]^{L\mu} \quad (50)$$

Introducing (50) in (40) we obtain:

$$ASEP = \frac{a}{\pi} \cdot \int_0^{\frac{\pi}{2}} M_\gamma \left(\frac{-b}{2 \sin^2 \theta} \right) \cdot d\theta = \frac{a}{\pi} \cdot \int_0^{\frac{\pi}{2}} \left[\frac{4\mu^2 h}{\left(\frac{b \cdot \bar{\gamma}}{2 \sin^2 \theta} + 2\mu h \right)^2 - (2\mu H)^2} \right]^{L\mu} \cdot d\theta \quad (51)$$

Now we seek upper bound for ASEP for coherent detection by introducing (34) in (42):

$$ASEP_{UB} = \frac{a}{\sqrt{2\pi b \cdot \bar{\gamma}}} \cdot \frac{(2\mu)^{2L \cdot \mu} \cdot h^{L \cdot \mu}}{\left(\frac{b \cdot \bar{\gamma}}{2} + 2\mu(h-H) \right)^{2L \cdot \mu - 0,5}} \cdot \frac{\Gamma(2L \cdot \mu - 0,5)}{\Gamma(2L \cdot \mu)} \cdot {}_2F_1 \left(L \cdot \mu, 2L \cdot \mu - 0,5; 2L \cdot \mu; \frac{-4\mu H}{\frac{b \cdot \bar{\gamma}}{2} + 2\mu(h-H)} \right) \quad (52)$$

Lower bound for ASEP can be obtained by introducing (34) in (43):

$$ASEP_{LB} = \frac{a}{\sqrt{2\pi b \cdot \bar{\gamma}}} \cdot \frac{(2\mu)^{2L \cdot \mu} \cdot h^{L \cdot \mu}}{\left(\frac{b \cdot \bar{\gamma}}{2} + 2\mu(h-H) \right)^{2L \cdot \mu - 0,5}} \cdot \frac{\Gamma(2L \cdot \mu - 0,5)}{\Gamma(2L \cdot \mu)} \cdot {}_2F_1 \left(L \cdot \mu, 2L \cdot \mu - 0,5; 2L \cdot \mu; \frac{-4\mu H}{\frac{b \cdot \bar{\gamma}}{2} + 2\mu(h-H)} \right) - \frac{a}{\sqrt{2\pi (b \cdot \bar{\gamma})^3}} \cdot \frac{(2\mu)^{2L \cdot \mu} \cdot h^{L \cdot \mu}}{\left(\frac{b \cdot \bar{\gamma}}{2} + 2\mu(h-H) \right)^{2L \cdot \mu - 1,5}} \cdot \frac{\Gamma(2L \cdot \mu - 1,5)}{\Gamma(2L \cdot \mu)} \cdot {}_2F_1 \left(L \cdot \mu, 2L \cdot \mu - 1,5; 2L \cdot \mu; \frac{-4\mu H}{\frac{b \cdot \bar{\gamma}}{2} + 2\mu(h-H)} \right) \quad (53)$$

5. Simulations and discussion of the results

For the purposes of simulations, in this section first we discuss ways for generation of κ - μ and η - μ RVs. Since we have $f_\gamma(\gamma)$, and since we can't obtain inverse $f_\gamma^{-1}(\gamma)$, we have to apply Accept-Reject method. So, our goal is to generate random numbers from a continuous κ - μ and η - μ distributions with probability distribution functions given by (9) and (20), respectively. Although this method begins with uniform random number generator (RNG), it requires additional RNG. Namely, we first generate a random number from a continuous

distribution with probability distribution function $g_\gamma(\gamma)$, satisfying $f_\gamma(\gamma) \leq C \cdot g_\gamma(\gamma)$, for some constant C and for all γ . A continuous Accept-Reject RNG proceeds as follows:

1. we choose $g_\gamma(\gamma)$;
2. we find a constant C such that $f_\gamma(\gamma) / g_\gamma(\gamma) \leq C$ for all γ ;
3. we generate a uniform random number U ;
4. we generate a random number V from $g_\gamma(\gamma)$;
5. if $C \cdot U \leq f_\gamma(V) / g_\gamma(V)$, we accept V ;
6. else, we reject V and return to step 3.

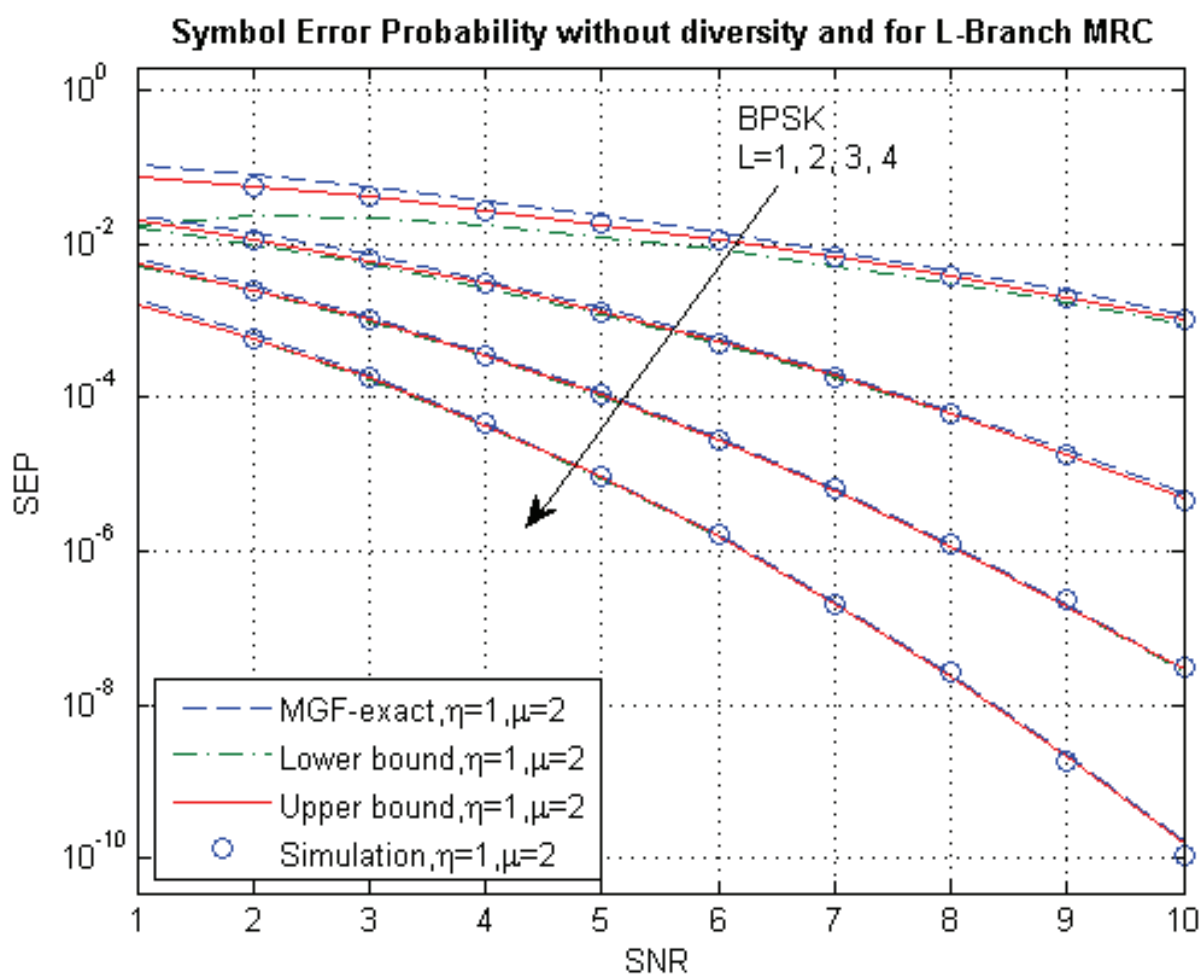


Fig. 14. Average symbol error probability for coherent BPSK, $L=1, 2, 3$ and 4

For efficiency of generation of random numbers V , we choose $g_\gamma(\gamma)$ as a exponential distribution. We find constant C so a condition $f_\gamma(\gamma) \leq C \cdot g_\gamma(\gamma)$ is satisfied. There is another, more efficient method for generation of κ - μ and η - μ RVs. For κ - μ and η - μ distributions, in accordance to (1) and (12) respectively, if $\mu = 0,5 \cdot q$, where q is an integer number, then it is possible to obtain κ - μ and η - μ distributed random numbers as a sum of squares of q Gaussian random numbers generated from a generator with adequate parameters. We designed simulator of κ - μ and η - μ based on outlines given above. We

used this simulator to generate samples of κ - μ and η - μ distributed instantaneous SNR. These samples are used to obtain outage probability as shown in Figs. 5-7 for κ - μ fading, and Figs. 8-10 for η - μ . As we can see from Figs. 7 and 10, there is not much need to increase number of combiner's branches beyond 4, because average SNR gained this way decreases for the same outage probability. On Figs. 11 and 13 ASEP for non-coherent BFSK has been depicted. Full lines represent theoretical ASEP curves given by (44) and (49), respectively. Markers on these figures represent values obtained by simulation. As we can see, theoretical and simulation results concur very well. Figs. 12 and 14 depict ASEP for coherent BPSK. On Fig. 12 we presented only simulation results (given by markers), and ASEP based on Q function upper-bound given by (47) (full lines). Here we can see some deviations between simulation results and theoretical expression. On Fig. 14 we presented 16 curves. Full lines represent curve of ASEP obtained by MGF (51); dashed curve represent ASEP based on Q function upper-bound given by (52); dot-dashed curve represent ASEP based on Q function lower-bound given by (53); markers represent curve obtained by simulation. We can see that simulation result concur with ASEP obtained by MGF (which was to be expected), while these two curves lay under upper-bound ASEP, and above lower-bound ASEP. Also, we can see that curves obtained by (52) and (53) are almost concurring with exact ASEP obtained by MGF.

6. Conclusion

Throughout this chapter we presented two general fading distributions, the κ - μ distribution and the η - μ distribution. Since we have placed accent on MRC in this chapter, we investigated properties of these distributions (we derived probability density functions for envelope, received power and instantaneous SNR; cumulative distribution function, n -th order moment and moment generating functions for instantaneous SNR), and derived relationships concerning distribution of SNR at MRC output (outage probability). Then we have analyzed average symbol error probability at MRC output in presence of κ - μ and η - μ distributed fading (we derived average symbol error probability for coherent and non-coherent detection; upper and lower bound of average symbol error probability for coherent). The results obtained clearly stated the obvious:

- for larger κ outage probability and symbol error probability were smaller for fixed μ , and fixed average SNR;
- for larger μ outage probability and symbol error probability were smaller for fixed, κ and fixed average SNR;
- for larger μ outage probability and symbol error probability were smaller for fixed, η and fixed average SNR;
- for η and $1/\eta$ we obtain the same results;
- for a greater number of MRC branches, outage probability and symbol error rate were smaller for fixed κ and μ , and for fixed η and μ .

Also, we gave some outlines for design of κ - μ and η - μ RNG.

Still, there is a lot of investigation in this field of engineering. Namely, scenarios for κ - μ and η - μ can be generalized in manner to assume that all clusters of multipath have dominant components with arbitrary powers and scattered components with different powers. Also,

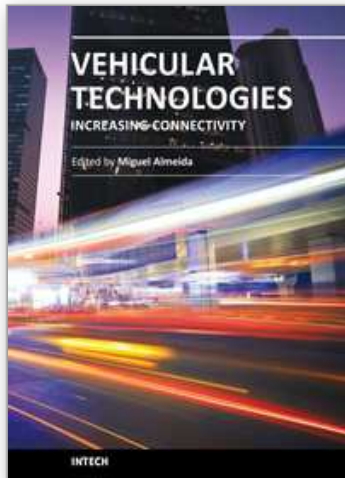
we can introduce nonlinearity in this fading model in the way Weibull did. Also, one should consider correlation among clusters of multipath. For suggested models, one should analyze combining performances: switched combining, equal-gain combining, maximal-ratio combining, general-switched combining, etc.

7. References

- Abramowitz, M.; Stegun, I.A. (1972). *Handbook of Mathematical Functions*, US Dept. of Commerce, National Bureau of Standards, Washington, DC
- Annamalai, W.A.; Tellambura, C. (2002). Analysis of hybrid selection/maximal-ratio diversity combiners with Gaussian errors, *IEEE Transactions on Wireless Communications*, Vol. 1, No. 3, July 2002, pp. 498 - 511
- Asplund, H.; Molisch, A.F.; Steinbauer, M. & Mehta, N.B. (2002), Clustering of Scatterers in Mobile Radio Channels - Evaluation and Modeling in the COST259 Directional Channel Model, *IEEE Proceedings of International Conference on Communications*, April-May 2002
- da Costa, D.B.; Yacoub, M.D., Fraidenraich, G. (2005). Second-order statistics for diversity-combining of non-identical, unbalanced, correlated Weibull signals, *SBMO/IEEE MTT-S Proceedings of International Conference on Microwave and Optoelectronics*, pp. 501 - 505, July 2005
- Fraidenraich, G.; Santos Filho, J.C.S.; Yacoub, M.D. (2005). Second-order statistics of maximal-ratio and equal-gain combining in Hoyt fading, *IEEE Communications Letters*, Vol. 9, No. 1, January 2005, pp. 19 - 21
- Fraidenraich, G.; Yacoub, M.D.; Santos Filho, J.C.S. (2005). Second-order statistics of maximal-ratio and equal-gain combining in Weibull fading, *IEEE Communications Letters*, Vol. 9, No. 6, Jun 2005, pp. 499 - 501
- Kim, S.W.; Kim, Y.G. ; Simon, M.K. (2003). Generalized selection combining based on the log-likelihood ratio, *IEEE Proceedings of International Conference on Communications*, pp. 2789 - 2794, May 2003
- Marcum, J.I. (1947). *A Statistical Theory of Target Detection by Pulsed Radar*, Project RAND, Douglas Aircraft Company, Inc., RA-15061, December 1947.
- Milišić , M.; Hamza, M.; Behlilović, N.; Hadžialić, M. (2009). Symbol Error Probability Analysis of L-Branch Maximal-Ratio Combiner for Generalized η - μ Fading, *IEEE Proceedings of International Conference on Vehicular Technology*, pp. 1-5, April 2009
- Milišić , M.; Hamza, M.; Hadžialić, M. (2008). Outage and symbol error probability performance of L-branch Maximal-Ratio combiner for generalized κ - μ fading, *IEEE Proceedings of International Symposium on Electronics in Marine - ELMAR*, pp. 231-236, September 2008
- Milišić , M.; Hamza, M.; Hadžialić, M. (2008). Outage Performance of L-branch Maximal-Ratio Combiner for Generalized κ - μ Fading, *IEEE Proceedings of International Conference on Vehicular Technology*, pp. 325-329, May 2008
- Milišić , M.; Hamza, M.; Hadžialić, M. (2009) BEP/SEP and Outage Performance Analysis of L-Branch Maximal-Ratio Combiner for κ - μ Fading, *International Journal of Digital Multimedia Broadcasting*, Vol.2009, 2009, 8 pages

- Prudnikov, A.P.; Brychkov, Yu.A.; Marichev, O.I. (1992). *Integrals and series : Direct Laplace Transforms*, Gordon and Breach Science Publishers
- Simon, M.K.; Alouini, M-S (2005). *Digital Communications over Fading Channels*, second edition, Wiley
- Stuber, G. L. (1996). *Principles of Mobile Communications*, Kluwer Academic Publishers, Norwell, MA.
- Yacoub, M. D. (2007). The κ - μ Distribution and the η - μ Distribution, *IEEE Antennas and Propagation Magazine*, Vol. 49, No. 1, February 2007, pp. 68 - 81

IntechOpen



Vehicular Technologies: Increasing Connectivity

Edited by Dr Miguel Almeida

ISBN 978-953-307-223-4

Hard cover, 448 pages

Publisher InTech

Published online 11, April, 2011

Published in print edition April, 2011

This book provides an insight on both the challenges and the technological solutions of several approaches, which allow connecting vehicles between each other and with the network. It underlines the trends on networking capabilities and their issues, further focusing on the MAC and Physical layer challenges. Ranging from the advances on radio access technologies to intelligent mechanisms deployed to enhance cooperative communications, cognitive radio and multiple antenna systems have been given particular highlight.

How to reference

In order to correctly reference this scholarly work, feel free to copy and paste the following:

Mirza Milišić, Mirza Hamza and Mesud Hadžialić (2011). Outage Performance and Symbol Error Rate Analysis of L-Branch Maximal-Ratio Combiner for κ - μ and η - μ Fading, Vehicular Technologies: Increasing Connectivity, Dr Miguel Almeida (Ed.), ISBN: 978-953-307-223-4, InTech, Available from:

<http://www.intechopen.com/books/vehicular-technologies-increasing-connectivity/outage-performance-and-symbol-error-rate-analysis-of-l-branch-maximal-ratio-combiner-for-and-fading>

INTECH

open science | open minds

InTech Europe

University Campus STeP Ri
Slavka Krautzeka 83/A
51000 Rijeka, Croatia
Phone: +385 (51) 770 447
Fax: +385 (51) 686 166
www.intechopen.com

InTech China

Unit 405, Office Block, Hotel Equatorial Shanghai
No.65, Yan An Road (West), Shanghai, 200040, China
中国上海市延安西路65号上海国际贵都大饭店办公楼405单元
Phone: +86-21-62489820
Fax: +86-21-62489821

© 2011 The Author(s). Licensee IntechOpen. This chapter is distributed under the terms of the [Creative Commons Attribution-NonCommercial-ShareAlike-3.0 License](#), which permits use, distribution and reproduction for non-commercial purposes, provided the original is properly cited and derivative works building on this content are distributed under the same license.

IntechOpen

IntechOpen